TISSUE ENGINEERING: Part A
Volume 20, Numbers 1 and 2, 2014

DOI: 10.1089/ten.tea.2013.0113

Fluorapatite Enhances Mineralization of Mesenchymal/Endothelial Cocultures

Xiaodong Wang, PhD,[1,2] Zhaocheng Zhang, PhD,[2] Syweren Chang, MS,[2] Agata Czajka-Jakubowska, PhD,[3] Jacques E. Nör, PhD,[2] Brian H. Clarkson, PhD,[2] Longxing Ni, PhD,[1] and Jun Liu, PhD[2]

In addition to the widely used mesenchymal stem cells (MSCs), endothelial cells appear to be a favorable cell source for hard tissue regeneration. Previously, fluorapatite was shown to stimulate and enhance mineralization of MSCs. This study aims to investigate the growth of endothelial cells on synthesized ordered fluorapatite surfaces and their effect on the mineralization of adipose-derived stem cells (ASCs) through coculture. Endothelial cells were grown on fluorapatite surfaces and characterized by cell counting, flow cytometry, scanning electron microscopy, and enzyme-linked immunosorbent assay (ELISA). Cells were then cocultured with ASCs and stained for alkaline phosphatase and mineral formation. Fibroblast growth factor (FGF) pathway perturbation and basic FGF (bFGF) treatment of the ASCs were also conducted to observe their effects on differentiation and mineralization of these cells. Fluorapatite surfaces showed good biocompatibility in supporting endothelial cells. Without a mineralization supplement, coculture with endothelial cells induced osteogenic differentiation of ASCs, which was further enhanced by the fluorapatite surfaces. This suggested a combined stimulating effect of endothelial cells and fluorapatite surfaces on the enhanced mineralization of ASCs. Greater amounts of bFGF release by endothelial cells alone or cocultures with ASCs stimulated by fluorapatite surfaces, together with FGF pathway perturbation and bFGF treatment results, suggested that the FGF signaling pathway may function in this process.

Introduction

Hard tissue regeneration using mesenchymal stem cells (MSCs) has been widely studied and continues attracting a great deal of attention.[1,2] More recently, adipose-derived stem cells (ASCs) have been well characterized and used in hard tissue engineering because of their availability, strong potential to undergo multiple differentiations,[3–5] and their genetic stability in long-term *in vitro* culture.[6]

Previously, it has been suggested that reciprocal interactions between MSCs and endothelial cells are pivotal in the bone regeneration process.[7] Although the cell fate of MSCs is affected by multiple factors, including exogenous soluble growth factors, cytokines, and external mechanical forces, the osteogenic differentiation of MSCs has been suggested to be closely related to their interaction with certain mature cell populations.[8] Still unclear is the precise role of endothelial cells on osteoblastic differentiation, but emerging studies have demonstrated that coculture of endothelial cells and mesenchymal precursor/stem cells stimulated the expression of bone phenotypic markers and enhanced the osteogenesis of cocultured mesenchymal cells.[9–11]

Recently, we reported that the ordered fluorapatite (OR-FA) surface when used as a potential implant coating, showed good biocompatibility with different cell lines, that is, dental pulp stem cells and osteoblast-like MG-63 cells and supported the long-term growth and differentiation of these cells.[12–14] This OR-FA surface stimulated, *in vitro*, the expression of a set of pro-osteogenic transcripts and bone mineralization phenotypic markers of ASCs, and consistently accelerated and enhanced *in vivo* mineralized tissue formation.[15] However, growth of endothelial cells on this OR-FA surface has never been tested. In an attempt to further establish this OR-FA surface as a potential scaffold or implant coating material for hard tissue regeneration and to mimic *in vivo* situations, this study was carried out to first determine the effects of OR-FA surfaces on the growth of endothelial cells and then to explore how the endothelial–mesenchymal coculture on the OR-FA surface will affect the osteogenic differentiation and mineralization of ASCs.

[1]Department of Operative Dentistry & Endodontics, School of Stomatology, Fourth Military Medical University, Xi'an, Shaanxi, P.R. China.
[2]Department of Cariology, Restorative Sciences and Endodontics, Dental School, University of Michigan, Ann Arbor, Michigan.
[3]Department of Maxillofacial Orthopaedics and Orthodontics, Poznan University of Medical Sciences, Poznan, Poland.

Materials and Methods

The hydrothermal synthesis and coating of the OR-FA crystal film on etched stainless steel (SSE) discs was carried out as previously described.[12,16]

Growth of human microvascular endothelial cells on OR-FA surfaces

Dermal-derived human microvascular endothelial cells (HMVECs; Lonza) were subcultured in the endothelial cell growth medium (EGM-2-MV BulletKit; Lonza) under standard culture conditions at 37°C in a humidified atmosphere containing 5% CO_2 and 95% air. The medium was changed every 2 days. Before cell seeding, the OR-FA and SSE surfaces were equilibrated with the culture medium for 2 h.

Cell proliferation. HMVECs were seeded at a density of 5×10^4 cells/mL onto OR-FA and SSE surfaces in 12-well culture plates. At day 1, 7, and 14, cells were trypsinized, stained with Trypan blue, and counted using a hemocytometer. Mean values of three samples per group were used for statistical analysis.

Flow cytometry analysis. Approximately 3×10^5 HMVECs were seeded on OR-FA and SSE surfaces in 60-mm culture dishes and allowed to grow to 80% confluence. After trypsinization, the cells were harvested, fixed in 75% ethanol at 4°C overnight. The cells were washed and resuspended in an RNase solution (20 μg/mL; Sigma) containing propidium iodide (25 μg/mL; Sigma) for 30 min and then subjected to flow cytometer analysis (Beckman Coulter). Triplicate cell samples were used for each group.

Scanning electron microscope observation. At day 1, 3, 7, and 14, HMVECs seeded on each surface were rinsed, fixed with 2.5% glutaraldehyde, dehydrated in ascending concentrations of ethanol, and vacuum dried. Specimens were gold-coated before observation, which was conducted on a scanning electron microscope (SEM) (Phillips XL30FEG; FEI Company).

Enzyme-linked immunosorbent assay. Supernatants of HMVECs grown on OR-FA and SSE surfaces at day 1, 3, 7, and 14 were collected after the medium was replaced with a basal medium 24 h before each time point. The concentration of the basic fibroblast growth factor (bFGF) was determined using an ELISA kit (R&D) according to the manufacturer's protocols, and calculated as picograms per milliliter. Triplicate samples from each group were used for statistical analysis.

Coculture of HMVECs with ASCs

HMVECs were grown in the EGM-2-MV medium as mentioned earlier. ASCs (Invitrogen) were subcultured in the reduced serum (2%) MesenPRO medium, (Invitrogen) under standard culture conditions at 37°C with 5% CO_2 and 95% air. When HMVECs and ASCs reached 80% confluence, both cells were collected and mixed at a ratio of 1:1. These cell mixtures were seeded on OR-FA and SSE surfaces in 12-well plates at a total density of 5×10^4/well. They were cultured in a 1:1 combination of the EGM-2-MV and MesenPRO coculture medium, which was changed every 2 days.

Fluorescence labeling of cocultured cells. HMVECs were labeled with CellTracker Red (CTR; Molecular Probes) and ASCs were labeled with CellTracker Green (CTG; Molecular Probes) according to the manufacturer's instructions. Briefly, the cells were trypsinized, washed in PBS, resuspended in a serum-free medium containing 5 μM CTG or CTR, and then incubated at 37°C for 40 min. Labeling was terminated by the addition of fetal bovine serum (FBS). Labeled HMVECs and ASCs, mixed at a 1:1 ratio, were seeded on OR-FA and SSE surfaces at a total density of 5×10^4 cells/well in 12-well plates. At day 1 and 3, the cells were washed with PBS, and counterstained with 300 nM DAPI (Molecular Probes) at 37°C for 5 min. Images were taken using the fluorescence microscope (Leica DMI3000 B).

Enzyme-linked immunosorbent assay. Supernatants of cocultures grown on OR-FA and SSE surfaces at day 1, 3, 7, and 14 were collected after the medium was replaced with the basal medium (without FBS) 24 h before each time point. The concentration of the bFGF was determined as described above.

Alkaline phosphatase staining. After 7 and 14 days of coculture, the specimens were washed with PBS, fixed in 4% paraformaldehyde for 30 min, and then incubated with 0.5 mg/mL napthol AS-MX phosphate (Sigma-Aldrich) and 1 mg/mL Fast red TR (Sigma-Aldrich) predissolved with 1% N,N dimethylformamide (Sigma-Aldrich) in 0.1 M Tris buffer (pH 9.2) at 37°C for 40 min. The specimens were counterstained in DAPI (300 nM; Molecular Probes) for 10 min, and washed in PBS before fluorescence imaging. Single cultures of HMVECs and ASCs served as controls. ImageJ (NIH) was used to compare the intensity of fluorescence staining between the different groups, and triplicate samples from each group were used for statistical analysis.

Alizarin red staining. At day 28, cells grown on the experimental surfaces were rinsed, fixed with 70% ethanol, and stained with Alizarin red (Osteogenesis Assay Kit; Millipore) according to the manufacturer's protocols. After staining, quantitative analysis was carried out through extraction of Alizarin red from stained samples using acetic acid. The Alizarin red concentration was calculated as micromoles per liter. Single cultures of HMVECs and ASCs on OR-FA and SSE surfaces as well as naked surfaces served as controls. Three to five samples from each group were used for quantification.

FGF signaling investigation

Perturbation with FGF receptor inhibitor. The FGF receptor (FGFR) was antagonized by the SU5402 compound, a specific inhibitor of the FGF signaling pathway. About 30 nM SU5402 (Millipore), which was dissolved in DMSO before a working solution was finally prepared with a medium, was added to the cultures of ASCs alone as well as cocultures of HMVECs and ASCs grown on OR-FA and SSE surfaces. These cells were also treated with supernatants collected from HMVECs grown on OR-FA and SSE surfaces for 7 days, with or without the addition of SU5402. Control groups were treated with media containing an equivalent amount of DMSO, with or without HMVEC supernatants. The specimens were processed for alkaline phosphatase (ALP) staining at day 7 as well as Alizarin red staining at day 21 as described above.

Treatment with bFGF. Briefly, bFGF was added to the culture medium at a concentration of 50 ng/mL. ASCs grown on OR-FA and SSE surfaces were treated with bFGF with or without SU5402 treatment. ASCs cultured without the addition of bFGF served as controls. At day 7 and 21, specimens were processed for ALP staining as well as Alizarin red staining as described above.

Western blotting. ASCs grown on OR-FA and SSE surfaces, treated with or without SU5402 and FGF, were collected for protein analysis. In brief, cell cultures at day 28 were washed with cold PBS and lysed in a cold NP-40 protein lysis buffer for 10 min on ice. Lysates were centrifuged at 12,000 rpm for 10 min at 4°C. Protein concentrations were determined by the Bradford method. Subsequently, proteins were separated by 15% sodium dodecyl sulfate–polyacrylamide gel electrophoresis (SDS-PAGE) and transferred electrophoretically to a nitrocellulose membrane. Nonspecific binding was blocked by immersing the membrane in 5% nonfat milk for 1 h at room temperature. The membrane was then incubated with the mouse antihuman osteocalcin (OCN) antibody (1:1000; Santa Cruz Biotechnology) at 4°C overnight, and further incubated with a secondary antibody conjugated with horseradish peroxidase anti-mouse IgG (1:5000; Santa Cruz Biotechnology) for 2 h, and developed using an enhanced chemiluminescent (ECL) kit (Thermo Scientific). β-actin was used as a loading control. Three separate cell lysates from the experimental substrate surfaces were used for the quantitative analysis of the optical band density of OCN expression by determining the ratio of OCN/β-actin using the ImageJ program (NIH). Relative band densities were compared with the band density of the control group.

Data analyses

The cell counting, enzyme-linked immunosorbent assay (ELISA), quantitative osteogenesis assay, and the ImageJ analysis results were analyzed statistically using GraphPad Prism 5 for one-way ANOVA (and *post hoc* pairwise comparisons) of an average of three to five replicates and significance was considered at $p < 0.05$. Data are expressed as mean ± standard deviation.

Results

Growth of HMVECs on OR-FA surfaces

Cell proliferation. At day 1, the total number of HMVECs on OR-FA and SSE surfaces was 3.1×10^4 and 3.3×10^4, respectively, and at day 7 the number was 11.5×10^4 and 13×10^4, and at day 14 the number was 41×10^4 and 44×10^4, respectively. There was no significant difference of the number of cells grown on the SSE and OR-FA surfaces ($p > 0.05$) (Fig. 1A).

Flow cytometry analysis. The cell cycle analysis revealed that HMVECs grown on OR-FA and SSE surfaces presented a similar percentage of cells in the S and G_2M phases. The proliferation index (PrI, $S+G_2M$) of the cells grown on OR-

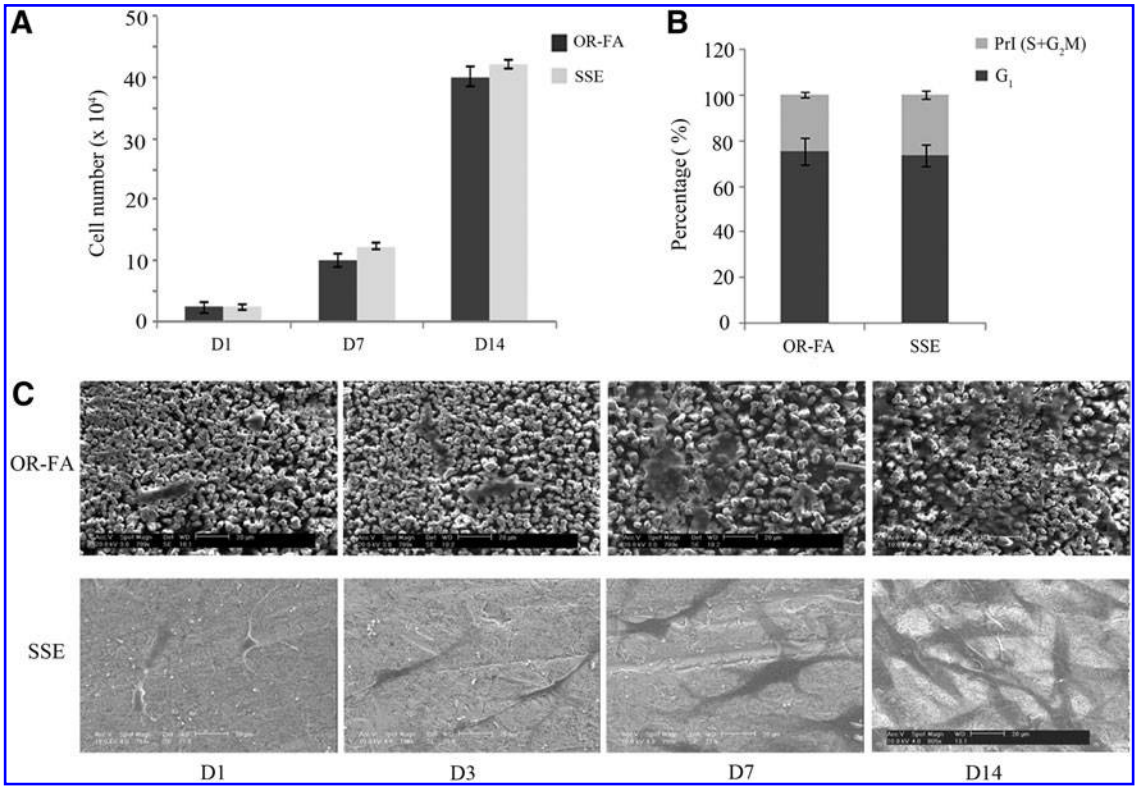

FIG. 1. Growth and characterization of HMVECs on OR-FA and etched SSE surfaces. Cell density of HMVECs on OR-FA and SSE surfaces (*$p < 0.05$) **(A)**. Cell cycle analysis of HMVECs grown on OR-FA and SSE surfaces for 2 days (%) **(B)**. Scanning electron microscope of HMVECs grown on OR-FA and SSE surfaces for 1, 3, 7, and 14 days **(C)**. OR-FA, ordered fluorapatite; SSE, stainless steel; HMVECs, human microvascular endothelial cells.

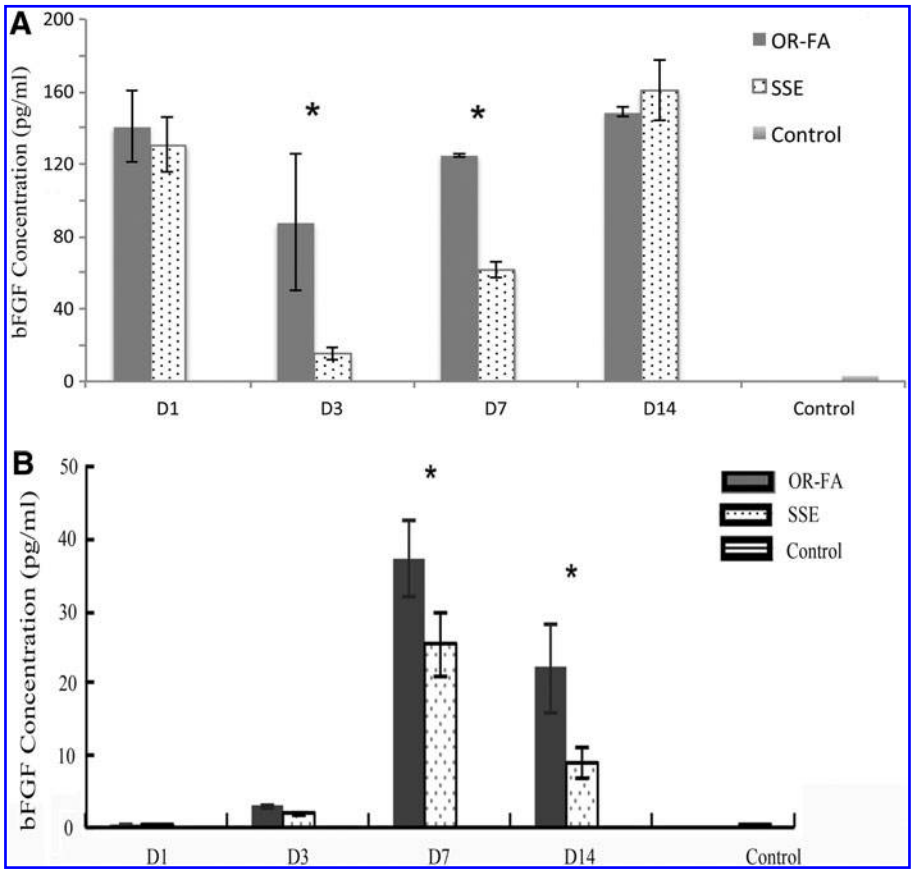

FIG. 2. ELISA of bFGF released by HMVECs grown alone **(A)** or cocultured with ASCs **(B)** on OR-FA and SSE surfaces (*$p < 0.05$). The medium incubated under the same condition served as control. Triplicate samples from each group were used for the statistical analysis. ASCs, adipose-derived stem cells; ELISA, enzyme-linked immunosorbent assay; bFGF, basic fibroblast growth factor.

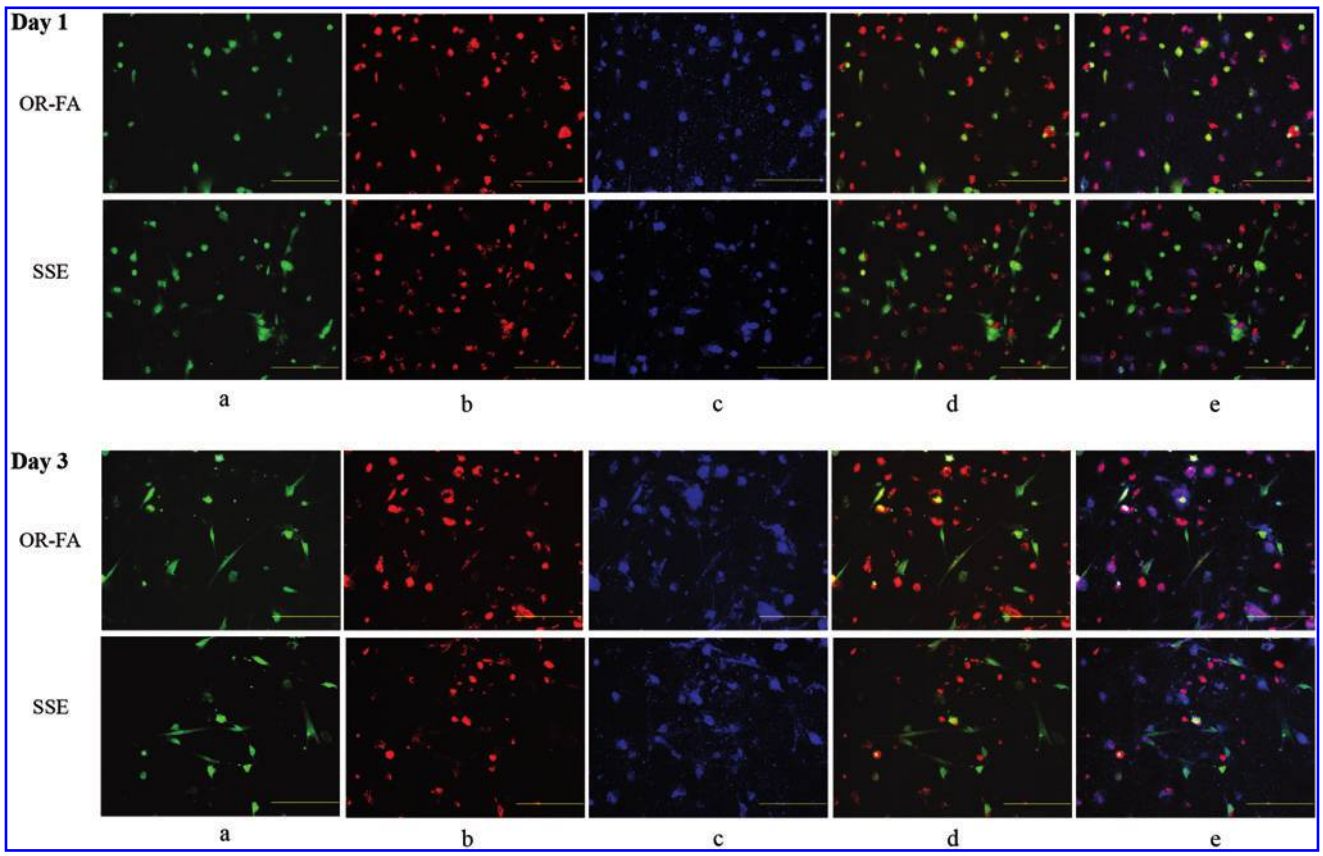

FIG. 3. Fluorescence microscopic observation of cocultured HMVECs and ASCs grown on OR-FA and SSE surfaces at day 1 and 3. **(a)** ASCs (CellTracker Green). **(b)** HMVECs (CellTracker Red). **(c)** DAPI stained nuclei. **(d)** Merged pictures of **(a, b)**. **(e)** Merged pictures of **(c, d)**. Scale bar: 200 μm. Color images available online at www.liebertpub.com/tea

FA and SSE surfaces was 24.8% and 25.9%, respectively. No significant difference was found between the two groups ($p > 0.05$) (Fig. 1B).

SEM observation. SEM observation suggested that the OR-FA surfaces showed good biocompatibility at different time points. HMVECs attached and flattened on both metal and FA surfaces; a greater number of cells were identified when the cells were cultured for a longer time on both surfaces (Fig. 1C).

Enzyme-linked immunosorbent assay. The released amount of bFGF by HMVECs grown on OR-FA surfaces was significantly higher than that on SSE surfaces after cell growth for 3 (87.82 pg/mL on OR-FA and 15.19 pg/mL on SSE) and 7 days (124.81 pg/mL on OR-FA and 61.56 pg/mL on SSE) ($p < 0.05$). However, there was no significant difference of the released bFGF by HMVECs grown on the two surfaces at day 14 (148.7 pg/mL on OR-FA and 161 pg/mL on SSE) ($p > 0.05$) (Fig. 2A).

Coculture of HMVECs with ASCs

Fluorescence observation. Fluorescence imaging indicated that both HMVECs and ASCs attached well and were evenly distributed on OR-FA and SSE surfaces. Some of the HMVECs and ASCs were in contact with each other. Clear cell boundaries and nuclei were observed in the cocultured HMVECs and ASCs on the two surfaces. In general, cocultured cells were more flattened on both surfaces at day 3 compared to those at day 1 (Fig. 3).

ELISA of bFGF. The released amount of bFGF by cocultures of HMVECs and ASCs grown on OR-FA surfaces was significantly higher compared with SSE surfaces at day 7

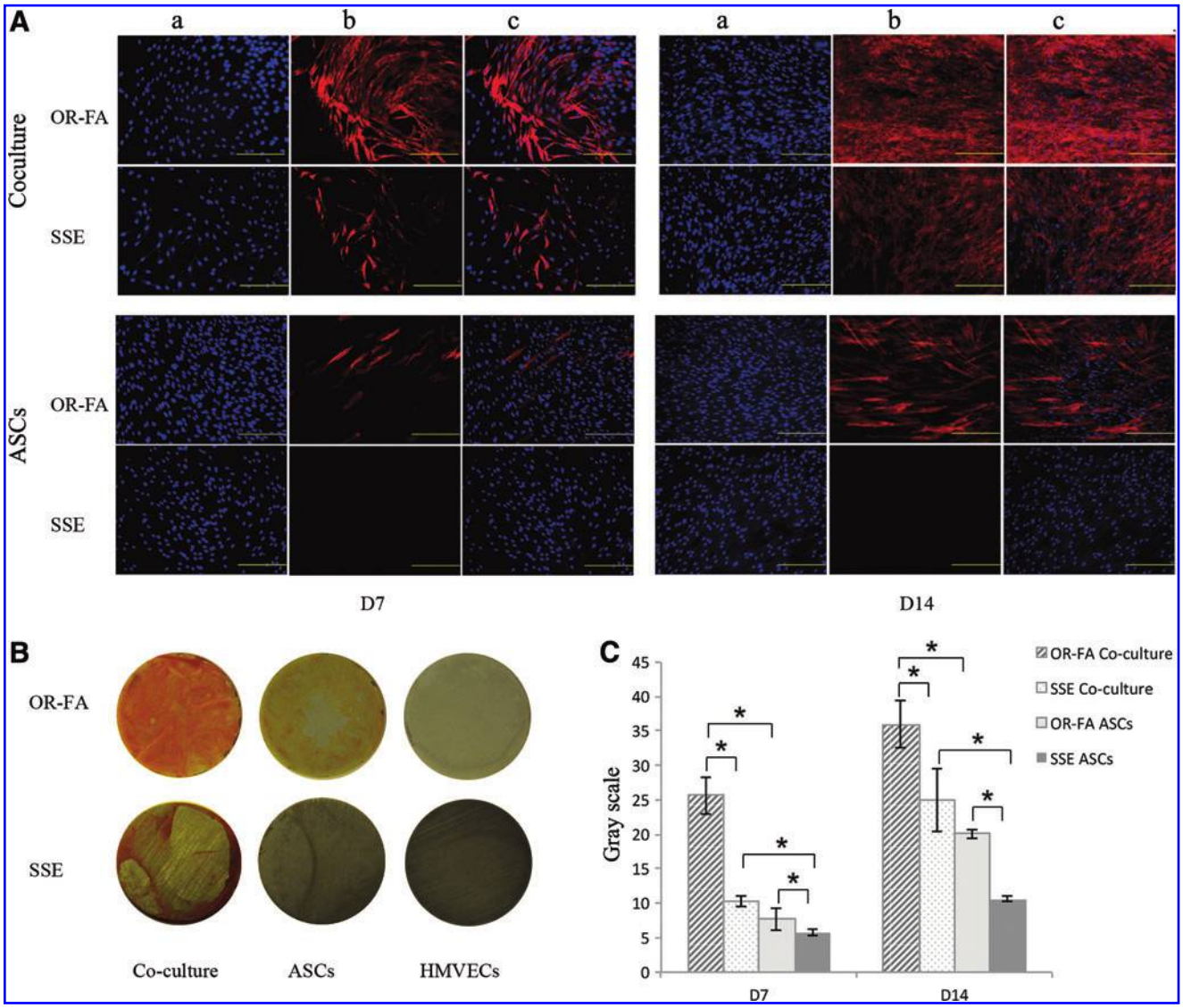

FIG. 4. ALP staining of cocultured HMVECs and ASCs grown on OR-FA and SSE surfaces. Fluorescent ALP staining of cocultured HMVECs and ASCs at day 7 and 14 **(A)**. **(a)** DAPI stained nuclei. **(b)** ALP staining (Fast red TR). **(c)** Merged pictures of **(a, b)**. Single culture of ASCs served as controls. Direct view of the entire discs of ALP staining at day 14 **(B)**. Quantitative analysis of fluorescent ALP staining intensity at day 7 and 14 **(C)**. *$p < 0.05$. Scale bar: 200 μm. ALP, alkaline phosphatase. Color images available online at www.liebertpub.com/tea

(37.5 pg/mL on OR-FA and 26.1 pg/mL on SSE) and 14 (22.0 pg/mL on OR-FA and 9.2 pg/mL on SSE) ($p < 0.05$). However, there was no significant difference between the two surfaces at day 1 and 3 ($p > 0.05$) (Fig. 2B).

ALP staining. At day 7, more ALP-positive cells with stronger staining were seen in cocultures grown on OR-FA surfaces compared with SSE surfaces (Fig. 4A). At day 14, ALP staining was much stronger on both surfaces compared to that at day 7. Similarly, staining intensity of cocultures was also more evident on OR-FA surfaces compared with SSE surfaces (Fig. 4A). These differences could be seen directly by viewing the entire surface of the discs (Fig. 4B). ImageJ analysis of fluorescence intensity further confirmed the difference between these groups (Fig. 4C).

Alizarin red staining. At day 28, cocultures grown on OR-FA and SSE surfaces both displayed positive Alizarin red staining. However, the staining intensity on OR-FA surfaces was much stronger compared with the SSE surfaces. The ASCs when grown alone on OR-FA surfaces showed a positive but weaker staining compared to that of the cocultures. Neither HMVECs alone grown on OR-FA or SSE surfaces nor ASCs alone on SSE surfaces displayed positive staining (Fig. 5A). A subsequent quantitative assay further confirmed these results (Fig. 5B).

FGF signaling investigation

Perturbation with FGFR inhibitor. At day 7, when ASCs were cultured alone or cocultured with HMVECs, ALP staining was much weaker on the SU5402-treated groups compared to the untreated groups on both OR-FA and SSE surfaces (Figs. 6A and 7A). Quantitative assays measuring the fluorescence intensity by ImageJ further confirmed these observations (Fig. 6B and 7B). With the addition of HMVEC supernatant, more ALP-positive cells were seen on both surfaces compared to the nonsupernatant groups when ASCs were cultured alone, with or without SU5402. A higher staining intensity was also identified on ASCs when grown on OR-FA surfaces than on SSE surfaces with or without HMVEC supernatants (Fig. 6A). This was consistent with subsequent fluorescence intensity measuring data (Fig. 6B). At day 21, the Alizarin red staining of ASCs alone and cocultures showed a similar staining pattern with their corresponding ALP staining (Figs. 8 and 9).

Treatment with bFGF. At day 7, ALP staining of ASCs was significantly stronger on bFGF-treated cells compared to untreated cells grown on both OR-FA and SSE surfaces. More ALP-positive cells could be seen on both surfaces when ASCs were treated with both SU5402 and bFGF compared to the control groups without FGF treatment (Fig. 6A). This observation was further confirmed by ImageJ analysis (Fig. 6B). At day 21, a similar staining pattern as well as the osteogenesis quantitative results, were found in these specimens after Alizarin red staining (Fig. 9).

Western blotting. After 28 days, the relative optical band density analysis showed OCN expression being significantly higher in cells grown on FA surfaces with FGF treatment, whereas the addition of SU5402 significantly inhibited the OCN expression (Fig. 10). No OCN expression was detected in the cells grown on SSE surfaces except for the cells being treated with bFGF.

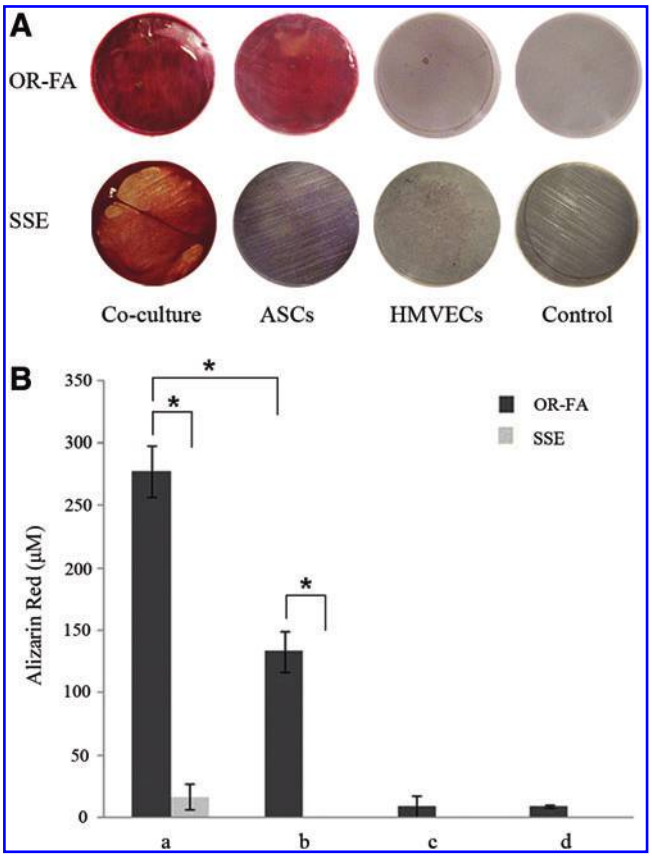

FIG. 5. Alizarin red staining of cocultured HMVECs and ASCs grown on OR-FA and SSE surfaces. Direct view of entire discs of Alizarin red staining of cells grown on OR-FA and SSE surfaces at day 28 **(A)**. Disc without cells served as controls. Quantitative analysis of Alizarin red staining **(B)**. **(a)** Cocultures of HMVECs and ASCs. **(b)** ASCs only. **(c)** HMVECs only. **(d)** Disc without cells, $*p < 0.05$. Color images available online at www.liebertpub.com/tea

Discussion

Previously, we have demonstrated that well-aligned OR-FA crystal coatings show good biocompatibility with MSCs and osteoblast-like cells.[12–15] In this study, we further investigated the initial attachment and growth of endothelial cells on the OR-FA films. The HMVECs' initial attachment, spreading, and proliferation observed by SEM was consistent with the cell counting data, showing good initial attachment and growth. These results, together with the flow cytometric data, which showed similar PrI between cells grown on metal and OR-FA surfaces, indicate that this OR-FA film presented biocompatible surfaces for the endothelial cells. Further, it suggested that the OR-FA surfaces were suitable for subsequent coculture experiments to explore potential roles of the surface and the cellular (endothelial signaling/endothelial–mesenchymal interaction) effects on osteogenic differentiation and mineralization of ASCs.

Most recently, we reported that the OR-FA structure induced osteogenic differentiation and mineralization of ASCs when

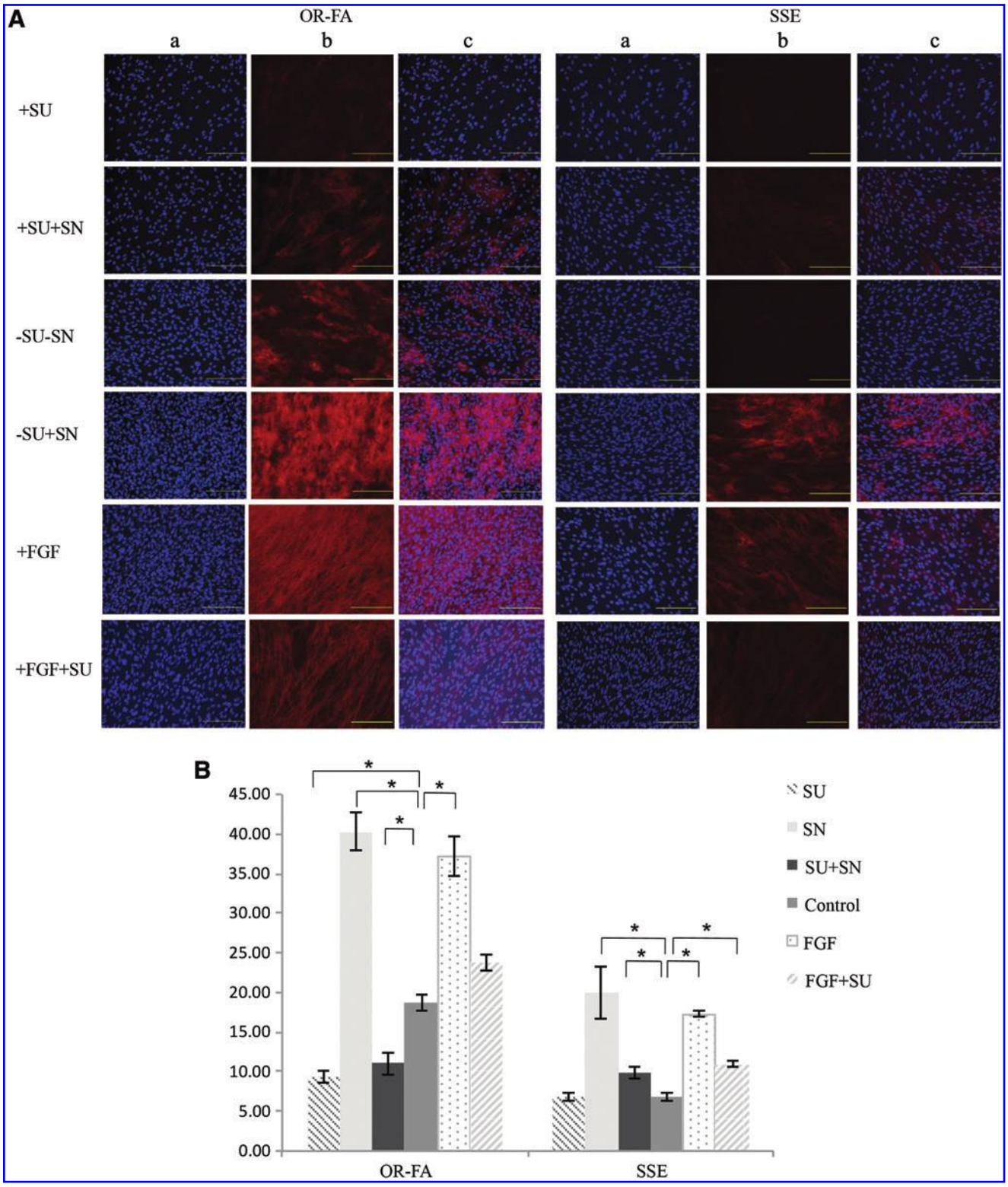

FIG. 6. ALP staining of ASCs grown on OR-FA and SSE surfaces, treated with/without bFGF, SU5402 (+SU/−SU), and HMVEC supernatant (+SN/−SN). Fluorescent ALP staining of ASCs at day 7 **(A)**. **(a)** DAPI stained nuclei. **(b)** ALP staining (Fast red TR). **(c)** Merged pictures of **(a** and **b)**. Quantification of fluorescent ALP staining intensity by ImageJ analysis **(B)**. Culture of ASCs without treatment served as controls. $*p < 0.05$. Scale bar: 200 μm. Color images available online at www.liebertpub.com/tea

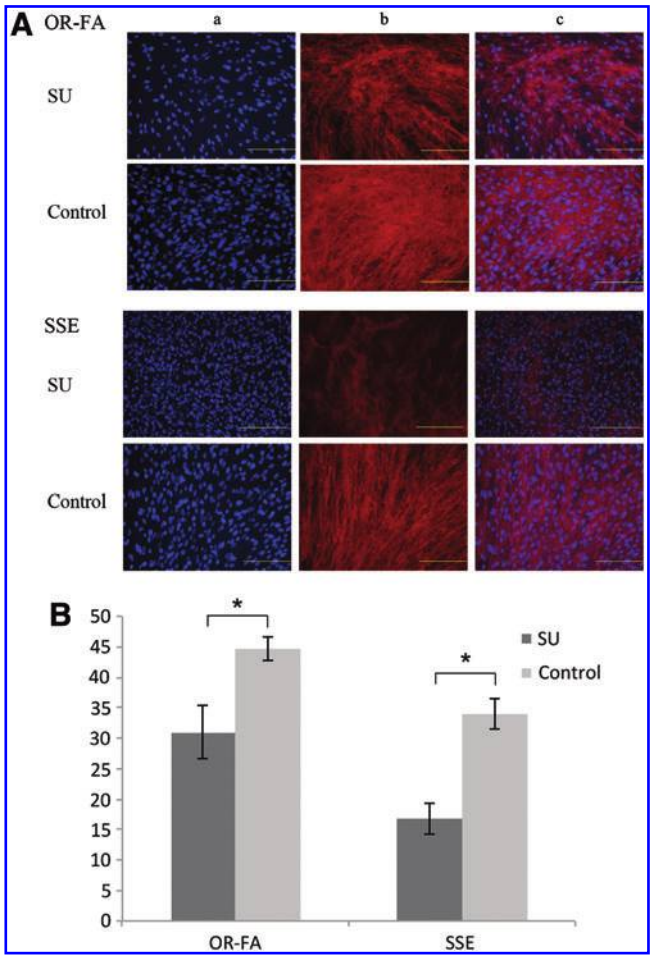

FIG. 7. ALP staining of cocultured HMVECs and ASCs grown on OR-FA and SSE surfaces, treated with/without SU5402 (SU) at day 7. Fluorescent ALP staining of cocultured HMVECs and ASCs with SU5402 (SU) treatment at day 7 **(A)**. **(a)** DAPI stained nuclei. **(b)** ALP staining (Fast red TR). **(c)** Merged pictures of **(a, b)**. Cocultures without treatment served as controls. Quantification of fluorescent ALP staining intensity by ImageJ analysis **(B)**. *$p < 0.05$. Scale bar: 200 μm. Color images available online at www.liebertpub.com/tea

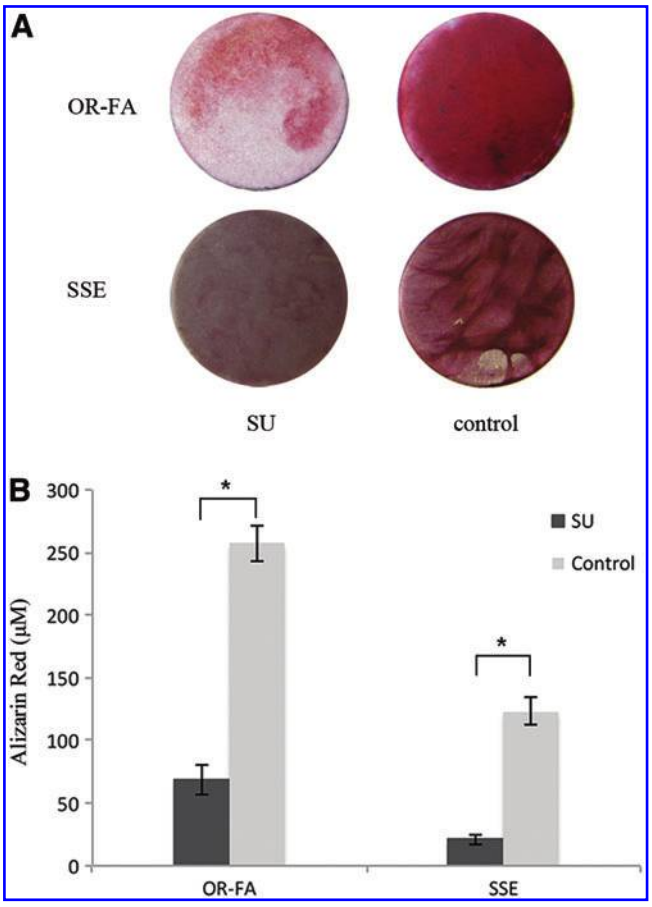

FIG. 8. Alizarin red staining of cocultured HMVECs and ASCs grown on OR-FA and SSE surfaces, treated with/without SU5402 (SU) at day 21. Direct view of entire discs of Alizarin red staining of cells grown on OR-FA and SSE surfaces at day 21 **(A)**. Cocultures without treatment served as controls. Quantitative analysis of Alizarin red staining **(B)**. *$p < 0.05$. Color images available online at www.liebertpub.com/tea

grown alone on these surfaces.[15] In the present study, what was most intriguing was the combined stimulating effect of the OR-FA surfaces and the endothelial/mesenchymal cell interaction on the MSC osteogenic differentiation and mineralization. Under physiological conditions and/or during the wound healing process, MSCs communicate and interact with the local vascular environment,[17,18] through either soluble molecules and extracellular matrices or the neighboring cells. In an indirect coculture study, MSC behavior was significantly affected by the addition of an endothelial cell-conditioned medium, which would contain a cocktail of endothelial growth factors.[19] It has also been shown that intercommunication and/or interaction between cells is dependent on gap junctions, and cell contact plays a crucial role in affecting various cellular activities, for example, the related cell proliferation and differentiation process.[20,21] It is still controversial whether the direct cell-to-cell contact is indispensable for the fate commitment of certain kinds of stem cells.[22–24] In this study, both the indirect and direct coculture models were used to investigate the endothelial cellular (endothelial signaling/endothelial–mesenchymal interaction) effects on the differentiation and mineralization of ASCs. In our study, athough the addition of HMVEC supernatants appeared to stimulate the differentiation and mineralization of ASCs grown on both the FA and SSE surfaces, the direct cocultures showed more evident osteogenic capabilities as indicated by the ALP staining, Alizarin red staining, and its subsequent quantitative analysis. Similarly, cocultures on the SSE surface also displayed positive ALP and Alizarin red staining, which was not seen when the ASCs were grown alone on the same surfaces. In the present study, the ASCs are considered the cells that have gone through osteogenic differentiation because, under normal culture conditions, HMVECs would not differentiate into the osteolineage cells,[8,11,20,21,25] and additionally, in our preliminary studies, we did not see any mineralization occurring when the HMVECs were grown alone on the FA surfaces (data not shown). Taken together, this would suggest that HMVECs stimulated both osteogenic differentiation of ASCs and the subsequent mineralization process, which may be mediated by both the released endothelial signals and/or the intimate interaction between these two kinds of cells. Consistent with this observation, human umbilical vein

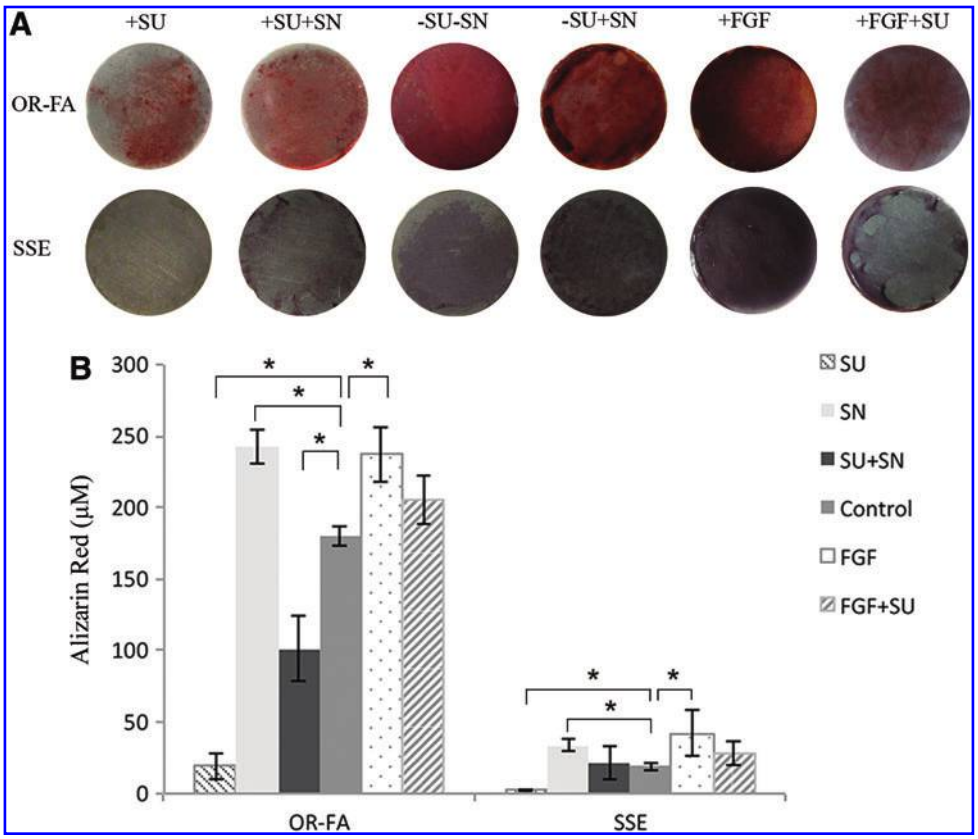

FIG. 9. Alizarin red staining of ASCs grown on OR-FA and SSE surfaces, treated with/without bFGF, SU5402 (+SU/−SU), and HMVEC supernatant (+SN/-SN). Direct view of entire discs of Alizarin red staining of cells grown on OR-FA and SSE surfaces at day 21 **(A)**. Quantitative analysis of Alizarin red staining **(B)**. Cultures of ASCs without treatment served as controls. *$p < 0.05$. Color images available online at www.liebertpub.com/tea

endothelial cells (HUVECs) have also been reported to promote osteogenesis of cocultured MSCs without mineralization supplements.[22] Mechanistically, OR-FA surfaces has been shown to stimulate expression of a set of pro-osteogenic transcripts and bone mineralization phenotypic markers from ASCs, but this does not occur when ASCs are grown on metal surfaces.[15] Thus, it appears that both the cellular (endothelial signaling/endothelial–mesenchymal interaction) involvement and the OR-FA crystal surfaces act cooperatively to affect the differentiation and mineralization of ASCs. This was further supported by the Alizarin red quantitative analysis. In this study, a 1:1 ratio of HMVEC:ASC was used in our coculture system, based on a previous study by Saleh *et al*.[21] In addition, Ma *et al.* studied the effects of different culture media and different ratios of human marrow stromal cells (HMSCs) and HUVECs on the osteogenic and angiogenic outcomes of the coculture. Their results showed that a HMSC/HUVEC coculture ratio of 1:1 appeared to be optimal.[26] However, most recently, a study did show that under dynamic culture conditions, coculture of human osteoblast-like cells with a low ratio of HUVECs on a copolymer scaffold significantly influenced the expression of osteogenic markers.[27] It would be interesting to explore, in the future, the effects of HMVEC seeding density, that is, the HMVEC:ASC ratio on the growth and differentiation of ASCs on the OR-FA and SSE surfaces.

The reciprocal interaction between endothelial and MSCs may have profound influence on cell fate, proliferation, differentiation, and subsequent angiogenesis and osteogenessis.[23–25] FGF signaling has been identified to regulate events in embryonic development, including mesenchymal–epithelial signaling and the development of multiple organ systems.[28,29] bFGF not only serves as a potent growth factor inducing angiogenesis, but plays an important role in the related osteogenesis process.[30,31] In our previous work, when ASCs were grown on OR-FA surfaces, in addition to BMP and TGFβ signaling pathways, the FGF pathway also appeared to be involved during the cell differentiation and mineralization process.[15] In this study, we had noticed a greater release of bFGF from HMVECs grown on OR-FA surfaces than on metal surfaces. We hypothesize that the topography and/or some intrinsic property of the OR-FA surfaces may, by recruiting certain growth factors or by interacting with the stem cells to generate potent inductive factors, stimulate the release of bFGF. The same pattern was also found in cocultures of ASCs and HMVECs. Furthermore, a significantly higher amount of bFGF was detected on the cocultures grown on FA surfaces compared to SSE surfaces at 14 days; however, the promoted bFGF release was only noticed on ASCs alone at earlier time points, but not as late as 14 days. Thus, the enhanced mineralization of the cocultures grown on the FA surfaces may be attributed to the stimulated and extended bFGF release, since mineralization would appear as early as day 14.[32] Interestingly, it was also noticed that the amount of released bFGF by cocultures was much lower than the release by HMVEC single cultures at the same time points. This could be explained by the much lower number of HMVECs used in the cocultures compared with single culture and also the consumption of released bFGF by the cocultured ASCs. Based on these results, an inhibitor specifically targeting the FGF signaling pathway was applied to investigate whether FGF signaling is involved in the crosstalk between endothelial cells and ASCs on OR-FA surfaces. As shown in this study, the FGFR inhibitor significantly inhibited the ALP activity, as well as, mineralized tissue formation of ASCs with or without cocultured HMVECs.

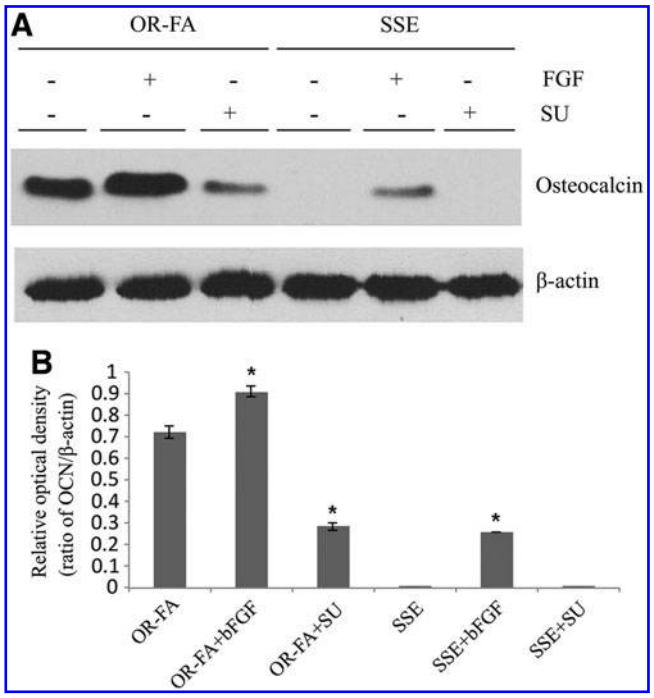

FIG. 10. Western blotting of OCN expression of ASCs grown on OR-FA and SSE surfaces, treated with/without bFGF and SU5402 (+SU/−SU) at day 28. OCN expression on ASCs grown on OR-FA and SSE surfaces, treated with/without bFGF and SU5402 (+SU/−SU) at day 28 **(A)**. β-actin served as loading control. Quantitative analysis of the optical band density of OCN expression by the ratio of OCN/β-actin using ImageJ program (NIH) **(B)**. Cells grown on two surfaces without any treatment served as controls. $*p < 0.05$. OCN, osteocalcin.

Besides the perturbation results, treatment with bFGF provided further evidence of the involvement of FGF signaling in the enhanced differentiation and mineralization of ASCs grown on these OR-FA surfaces, which were supported by our quantitative studies on ALP activities and mineral nodule formation. As one of the most abundant noncollagenous proteins found in mineralized adult bone, OCN binds strongly with the mineral crystal in a calcium-dependent manner.[33] It serves as one of the specific markers of late-stage osteoblast differentiation.[12,15] In this study, consistent with ALP and Alizarin red staining results, OCN expression was significantly stimulated by FGF treatment in cells grown on OR-FA surfaces and induced in cells grown on SSE surfaces, whereas the FGF inhibitor significantly inhibited the OCN expression. Without bFGF treatment, although OR-FA surfaces but not SSE surfaces could still induce the OCN expression, inhibition of FGF signaling significantly reduced this OCN expression. This provided important evidence that the ASC osteogenic differentiation and mineralization was probably mediated, at least in part, through the activation of the FGF signaling pathway. Within the limitation of the present study, the bFGF signal is suggested to be involved in the osteogenic differentiation of ASCs promoted by OR-FA surfaces as well as by the endothelial–mesenchymal interaction. Moreover, the ALP inhibition of ASCs by this FGFR inhibitor could be partially rescued by the HMVEC supernatant and also the FGF treatment. This further suggests a combined stimulating effect of endothelial origin signaling/endothelial–mesenchymal interaction and OR-FA surface on enhanced ASC differentiation and mineralization.

Conclusions

Ordered FA surfaces showed good biocompatibility for supporting the growth of endothelial cells. Coculture with HMVECs significantly promoted osteogenic differentiation and mineralization of ASCs, which was particularly enhanced by OR-FA surfaces. This may suggest a combined stimulating effect of endothelial origin signaling/endothelial–mesenchymal interaction and OR-FA surface on enhanced ASC differentiation and mineralization. The osteogenic differentiation of ASCs stimulated by OR-FA surfaces as well as endothelial cells has been shown to be mediated through, but probably not only, the FGF signaling pathway. Still a fascinating and unsolved puzzle: how could the FA surfaces or the endothelial signals induce the differentiation and mineralization of MSCs without any osteogenic supplement? Studies on details of the involvement of the FGF signaling pathway, for example, identification of signaling molecules acting on tissue-specific FGFRs and identification of other pathways that are associated or activated by FGF/FGFR signaling during these processes need to be carried out in the future. This work supports our previous observations of using the FA films as a scaffold or implant coating material for various dental and orthopedic applications.

Acknowledgment

This study was supported by the NIH grant DE020983.

Disclosure Statement

No competing financial interests exist.

References

1. Farre-Guasch, E., Marti-Page, C., Hernadez-Alfaro, F., Klein-Nulend, J., and Casals, N. Buccal fat pad, an oral access source of human adipose stem cells with potential for osteochondral tissue engineering: an *in vitro* study. Tissue Eng Part C Methods **16,** 1083, 2010.
2. Monaco, E., Bionaz, M., Hollister, S.J., and Wheeler, M.B. Strategies for regeneration of the bone using porcine adult adipose-derived mesenchymal stem cells. Theriogenology **75,** 1381, 2011.
3. Zuk, P.A., Zhu, M., Mizuno, H., Huang, J., Futrell, J.W., Katz, A.J., *et al.* Multilineage cells from human adipose tissue: implications for cell-based therapies. Tissue Eng **7,** 211, 2001.
4. Gimble, J.M., Katz, A.J., and Bunnell, B.A. Adipose derived stem cells for regenerative medicine. Circ Res **100,** 1249, 2007.
5. Meza-Zepeda, L.A., Noer, A., Dahl, J.A., Micci, F., Myklebost, O., and Collas, P. High resolution analysis of genetic stability of human adipose tissue stem cells cultured to senescence. J Cell Mol Med **12,** 553, 2008.
6. Dahl, J.A., Duggal, S., Coulston, N., Millar, D., Melki, J., Shahdadfar, A., *et al.* Genetic and epigenetic instability of human bone marrow mesenchymal stem cells expanded in autologous serum or fetal bovine serum. Int J Dev Biol **52,** 1033, 2008.
7. Laranjeira, M.S., Fernandes, M.H., and Monteiro, F.J. Reciprocal induction of human dermal microvascular endothelial cells and human mesenchymal stem cells: time-dependent profile in a co-culture system. Cell Prolif **45,** 320, 2012.

8. Kaigler, D., Krebsbach, P.H., West, E.R., Horger, K., Huang, Y.C., and Mooney, D.J. Endothelial cell modulation of bone marrow stromal cell osteogenic potential. FASEB J **19,** 665, 2005.
9. Guillotin, B., Bourget, C., Remy-Zolgadri, M., Bareille, R., Fernandez, P., Conrad, V., *et al.* Human primary endothelial cells stimulate human osteoprogenitor cell differentiation. Cell Physiol Biochem **14,** 325, 2004.
10. Unger, R.E., Sartoris, A., Peters, K., Motta, A., Migliaresi, C., Kunkel, M., *et al.* Tissue-like self-assembly in co-cultures of endothelial cells and osteoblasts and the formation of microcapillarylike structures on three-dimensional porous biomaterials. Biomaterials **28,** 3965, 2007.
11. Li, H., Daculsi, R., Grellier, M., Bareille, R., Bourget, C., and Amedee, J. Role of neural-cadherin in early osteoblastic differentiation of human bone marrow stromal cells co-cultured with human umbilical vein endothelial cells. Am J Physiol Cell Physiol **299,** C422, 2010.
12. Liu, J., Jin, T.C., Chang, S., Czajka-Jakubowska, A., Zhang, Z., Nör, J.E., *et al.* The effect of novel fluorapatite surfaces on osteoblast-like cell adhesion, growth, and mineralization. Tissue Eng Part A **16,** 2977, 2010.
13. Liu, J., Jin, T.C., Chang, S., Czajka-Jakubowska, A., and Clarkson, B.H. Adhesion and growth of dental pulp stem cells on enamel-like fluorapatite surfaces. J Biomed Mater Res A **96,** 528, 2011.
14. Wang, X.D., Jin, T.C., Chang, S., Zhang, Z.C., Czajka-Jakubowska, A., Nör, J.E., *et al. In vitro* differentiation and mineralization of dental pulp stem cells (DPSCs) on enamel-like fluorapatite surfaces. Tissue Eng Part C **18,** 821, 2012.
15. Liu, J., Wang, X.D., Jin, Q.M., Jin, T.C., Chang, S., Zhang, Z.C., *et al.* The stimulation of adipose-derived stem cell differentiation and mineralization by ordered rod-like fluorapatite coatings. Biomaterials **33,** 5036, 2012.
16. Chen, H.F., Tang, Z.Y., Liu, J., Sun, K., Chang, S.R., Peters, M.C., *et al*. A cellular synthesis of a human enamel-like microstructure. Adv Mater **18,** 1846, 2006.
17. Shi, S., and Gronthos, S. Perivascular niche of postnatal mesenchymal stem cells in human bone marrow and dental pulp. J Bone Miner Res **18,** 696, 2003.
18. Castrechini, N.M., Murthi, P., Gude, N.M., Erwich, J.J.H.M., Gronthos, S., Zannettino, A., *et al.* Mesenchymal stem cells in human placental chorionic villi reside in a vascular Niche. Placenta **31,** 203, 2010.
19. Saleh, F.A., Whyte, M., Ashton, P., and Genever, P.G. Regulation of mesenchymal stem cell activity by endothelial cells. Stem Cells Dev **20,** 391, 2011.
20. Villars, F., Guillotin, B., Amedee, T., Dutoya, S., Bordenave, L., Bareille, R., *et al.* Effect of HUVEC on human osteoprogenitor cell differentiation needs heterotypic gap junction communication. Am J Physiol Cell Physiol **282,** C775, 2002.
21. Grellier, M., Ferreira-Tojais, N., Bourget, C., Bareillke, R., Guillemot, F., and Amédée, J. Role of vascular endothelial growth factor in the communication between human osteoprogenitors and endothelial cells. J Cell Biochem **106,** 390, 2009.
22. Bidarra, S.J., Barrias, C.C., Barbosa, M.A., Soares, R., Amédée, J., and Granja, P.L. Phenotypic and proliferative modulation of human mesenchymal stem cells via crosstalk with endothelial cells. Stem Cell Res **7,** 186, 2011.
23. Ball, S.G., Shuttleworth, A.C., and Kielty, C.M. Direct cell contact influences bone marrow mesenchymal stem cell fate. Int J Biochem Cell Biol **36,** 714, 2004.
24. Ern, C., Krump-Konvalinkova, V., Docheva, D., Schindler, S., Rossmann, O., Böcker, W., *et al*. Interactions of human endothelial and multipotent mesenchymal stem cells in cocultures. Open Biomed Eng J **4,** 190, 2010.
25. Guillotin, B., Bareille, R., Bourget, C., Bordenave, L., and Amédée, J. Interaction between human umbilical vein endothelial cells and human osteoprogenitors triggers pleiotropic effect that may support osteoblastic function. Bone **42,** 1080, 2008.
26. Ma, J., van den Beucken, J.J., Yang, F., Both, S.K., Cui, F.Z., Pan, J., and Jansen, J.A. Coculture of osteoblasts and endothelial cells: optimization of culture medium and cell ratio. Tissue Eng Part C Methods **17,** 349, 2011.
27. Xing, Z., Xue, Y., Finne-Wistrand, A., Yang, Z.Q., and Mustafa, K. Copolymer cell/scaffold constructs for bone tissue engineering: co-culture of low ratios of human endothelial and osteoblast-like cells in a dynamic culture system. J Biomed Mater Res A **101,** 1113, 2013.
28. Yamaguchi, T.P., Harpal, K., Henkemeyer, M., and Rossant, J. fgfr-1 is required for embryonic growth and mesodermal patterning during mouse gastrulation. Genes Dev **8,** 3032, 1994.
29. De Moerlooze, L., Spencer-Dene, B., Revest, J.M., Hajihosseini, M., Rosewell, I., and Dickson, C. An important role for the IIIb isoform of fibroblast growth factor receptor 2 (FGFR2) in mesenchymal-epithelial signalling during mouse organogenesis. Development **127,** 483, 2000.
30. Rodan, S.B., Wesolowski, G., Thomas, K.A., Yoon, K., and Rodan, G.A. Effects of acidic and basic fibroblast growth factors on osteoblastic cells. Connect Tissue Res **20,** 283, 1989.
31. Pepper, M.S., Ferrara, N., Orci, L., and Montesano, R. Potent synergism between vascular endothelial growth factor and basic fibroblast growth factor in the induction of angiogenesis *in vitro*. Biochem Biophys Res Commun **189,** 824, 1992.
32. Liu, J., Jin, T., Ritchie, H.H., Smith, A.J., and Clarkson, B.H. *In vitro* differentiation and mineralization of human dental pulp cells induced by dentin extract. In Vitro Cell Dev Biol Anim **41,** 232, 2005.
33. Hoang, Q.Q., Sicheri, F, Howard, A.J., and Yang, D.S. Bone recognition mechanism of porcine osteocalcin from crystal structure. Nature **425,** 977, 2003.

Address correspondence to:
Jun Liu, PhD
Department of Cariology
Restorative Sciences and Endodontics
2310 I Dental School
University of Michigan
1011 N. University Avenue
Ann Arbor, MI 48109

E-mail: junlc@umich.edu

Longxing Ni, PhD
Department of Operative Dentistry & Endodontics
School of Stomatology
Fourth Military Medical University
Xi'an 710032
Shaanxi
P.R. China

E-mail: nilx2007@gmail.com

Received: February 13, 2013
Accepted: July 3, 2013
Online Publication Date: September 23, 2013

This article has been cited by:

1. D. Clark, X. Wang, S. Chang, A. Czajka-Jakubowska, B. H. Clarkson, J. Liu. 2015. VEGF promotes osteogenic differentiation of ASCs on ordered fluorapatite surfaces. *Journal of Biomedical Materials Research Part A* **103**:2, 639-645. [Crossref]
2. Yusuke Suzuki, Makoto Hayashi, Natsuko Tanabe, Takuya Yasukawa, Yoriyuki Hirano, Shozo Takagi, Laurence C. Chow, Naoto Suzuki, Bunnai Ogiso. 2015. Effect of a novel fluorapatite-forming calcium phosphate cement with calcium silicate on osteoblasts in comparison with mineral trioxide aggregate. *Journal of Oral Science* **57**:1, 25-30. [Crossref]
3. T. Guo, Y. Li, G. Cao, Z. Zhang, S. Chang, A. Czajka-Jakubowska, J.E. Nör, B.H. Clarkson, J. Liu. 2014. Fluorapatite-modified Scaffold on Dental Pulp Stem Cell Mineralization. *Journal of Dental Research* **93**:12, 1290-1295. [Crossref]